JOURNAL OF MORPHOLOGY 269:349–364 (2008)

The Morphology and Evolutionary Significance of the Ciliary Fields and Musculature Among Marine Bryozoan Larvae

Scott Santagata*

Smithsonian Marine Station, Fort Pierce, Florida 34949

ABSTRACT Despite the embryological and anatomical disparities present among lophotrochozoan phyla, there are morphological similarities in the cellular arrangements of ciliated cells used for propulsion among the nonfeeding larval forms of kamptozoans, nemerteans, annelids, mollusks, and bryozoans. Evaluating whether these similarities are the result of convergent selective pressures or a shared (deep) evolutionary history is hindered by the paucity of detailed cellular information from multiple systematic groups from lesser-known, and perhaps, basal evolutionary phyla such as the Bryozoa. Here, I compare the ciliary fields and musculature among the major morphological grades of marine bryozoan larvae using light microscopy, SEM, and confocal imaging techniques. Sampling effort focused on six species from systematic groups with few published accounts, but an additional four well-known species were also reevaluated. Review of the main larval types among species of bryozoans and these new data show that, within select systematic groups of marine bryozoans, there is some conservation of the cellular arrangement of ciliary fields and larval musculature. However, there is much more morphological diversity in these structures than previously documented, especially among nonfeeding ctenostome larval types. This structural and functional diversification reflects species differences in the orientation of the apical disc during swimming and crawling behaviors, modification of the presumptive juvenile tissues, elongation of larval forms in the aboral–oral axis, maximizing the surface area of cell types with propulsive cilia, and the simplification of ciliary fields and musculature within particular lineages due to evolutionary loss. Considering the embryological origins and functional plasticity of ciliated cells within bryozoan larvae, it is probable that the morphological similarities shared between the coronal cells of bryozoan larvae and the prototrochal cells of trochozoans are the result of convergent functional solutions to swimming in the plankton. However, this does not rule out cell specification pathways shared by more closely related spiralian phyla. Overall, among the morphological grades of larval bryozoans, the structural variation and arrangement of the main cell groups responsible for ciliary propulsion have been evolutionarily decoupled from the more divergent modifications of larval musculature. The structure of larval ciliary fields reflects the functional demands of swimming and substrate exploration behaviors before metamorphosis, but this is in contrast to the morphology of larval musculature and presumptive juvenile tissues that are linked to macroevolutionary differences in morphogenetic movements during metamorphosis. J. Morphol. 269:349–364, 2008.

KEY WORDS: Bryozoa; larva; musculature; cilia; *Bugula*; *Celleporaria*; *Schizoporella*; *Sundanella*; *Aeverrillia*; *Nolella*; *Amathia*; *Crisia*; F-actin; Lophotrochozoa

INTRODUCTION

The diverse forms of marine invertebrate larvae serve as unique tools for understanding the evolutionary and ecological relationships among multicellular animals. One main question regarding larval form is whether similarities in larval morphology are phylogenetically linked or if the body plans of larvae are free to evolve, arriving at similar morphologies based on convergent selective pressures (McEdward and Janies, 1993; Strathmann and Eernisse, 1994; Wray, 2002; Santagata, 2004; Raff and Byrne, 2006). Several investigations have concluded that the transition from a feeding to a nonfeeding larva (or vice versa) is a common evolutionary switch among marine invertebrates having no significant phylogenetic signal (Hart et al., 1997; Duda and Palumbi, 1999; Nützel et al., 2006). However, in some cases, the structure of larval and presumptive juvenile tissues is conserved among closely related species (Lyke et al., 1983; Santagata and Zimmer, 2002).

Perhaps the greatest disparity of larval and adult body plans exists within and among the phyla of the Lophotrochozoa. Despite numerous advances in molecular phylogenetic markers and analyses, the relationships among the annelids, mollusks, nemerteans, sipunculids, and the "lophophorates" remain

This article contains supplementary material available via the Internet at http://www.interscience.wiley.com/jpages/0362-2525/suppmat.

Contract grant sponsor: Smithsonian Postdoctoral Fellowship.

*Correspondence to: Scott Santagata, Smithsonian Environmental Research Center, Marine Invasions Laboratory, 647 Contees Wharf Road, Edgewater, MD 21037. E-mail: scott.santagata@gmail.com

Published online 25 October 2007 in
Wiley InterScience (www.interscience.wiley.com)
DOI: 10.1002/jmor.10592

largely unresolved (Halanych, 2004). Furthermore, recent advances in cytological comparisons with ubiquitous probes (McDougall et al., 2006), confocal microscopy (Jenner, 2006), and the expression of conserved developmental genes (Tessmar-Raible and Arendt, 2003) have clearly improved our understanding of the developmental mechanisms behind similarities in larval anatomy, but often fail to document the variability of these traits within phyla. Currently, taxonomic sampling for these investigations within the Lophotrochozoa is dominated by species of mollusks and annelids, whose spiralian development and trochophore-originated larval forms do not reflect the diversity exhibited by the lophotrochozoans as a whole. Since larvae of other lophotrochozoan phyla such as the nemerteans and sipunculids also share trochophore-like characteristics (Maslakova et al., 2004a,b; Wanninger et al., 2005), future research should focus on the more divergent larval forms present among the phoronids, brachiopods, and bryozoans. Some recent work has integrated traditional histological research with insights from more recent microscopic methods among phoronids and brachiopods (Freeman and Martindale, 2002; Santagata, 2002); however, the anatomy of bryozoan larvae remains largely defined by ultrastructural methods (Reed, 1991; Zimmer and Woollacott, 1993).

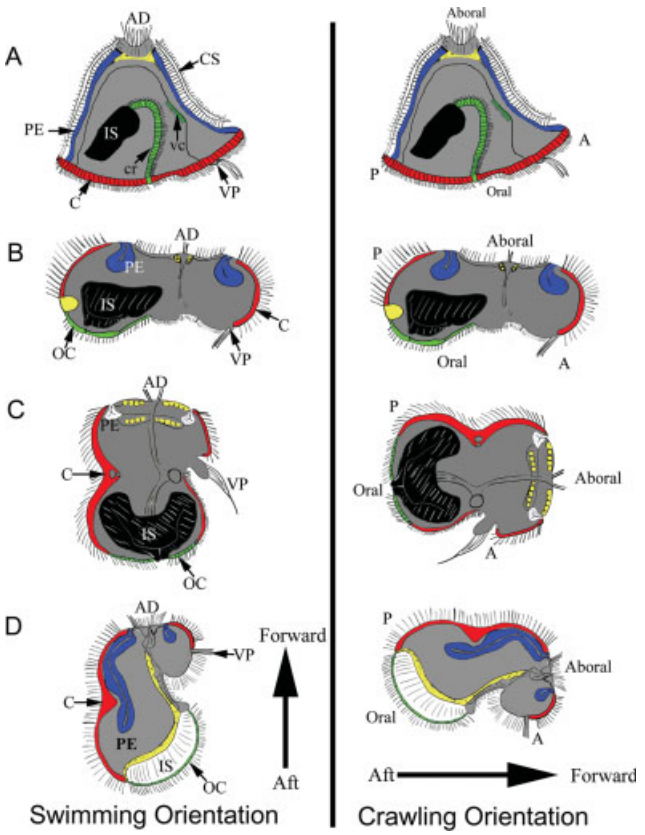

Fig. 1. Main anatomical differences among some of the better described larval forms of marine bryozoans. Also depicted is the orientation of the larva during swimming and crawling behaviors. Tissues shaded in blue (pallial epithelium) and black (internal sac) contribute the cystid at metamorphosis. In species where one of these tissues does not contribute to the ancestrula at metamorphosis, either the pallial epithelium (PE) or internal sac (IS) is uncolored. Tissues shaded in yellow are groups of undifferentiated cells that form the polypide after metamorphosis. Cells shaded in red constitute the coronal cell ring (C) mainly used for ciliary propulsion. Cells shaded in green either form the ciliated ridges (CR) and other ciliated cells within the vestibule (VC, only a subset are figured) found in species with a planktotrophic larva or are the oral ciliated cells (OC) of some nonfeeding larval types. Structures found in all forms include the apical disc (AD) and vibratile plume (VP). **A:** Cyphonautes larva of *Membranipora membranacea* (redrawn and modified from Stricker et al., 1988a). This feeding larval type is covered by bivalved shells (CS). **B:** The coronate larva of *Celleporaria brunnea* (from data in Santagata and Zimmer, 2000). **C:** The buguliform larva of *Bugula neritina* (redrawn and modified from Reed and Woollacott, 1982). **D:** The vesiculariform larva of *Amathia vidovici* (redrawn and modified from Zimmer and Woollacott, 1993).

Bryozoan Larval Morphology

Detailed morphological descriptions of bryozoan larvae have been limited to a few species (e.g., Woollacott and Zimmer, 1971; d'Hondt, 1973; Reed and Cloney, 1982a; Stricker et al., 1988a; Zimmer and Woollacott, 1989a; Zimmer and Reed, 1994). This has hindered the ability of investigators to form general hypotheses as to the evolutionary significance of larval traits (although see Zimmer and Woollacott, 1993). However, these reports have established the cell terminology that can be applied to the investigation of any bryozoan larva.

The most familiar types of bryozoan larvae are the feeding cyphonautes type (Kupelwieser, 1905) present in both uncalcified (ctenostome) and calcified (cheilostome) gymnolaemate bryozoans and the various forms of nonfeeding larval types present in the cyclostome, ctenostome, and cheilostome grades of marine bryozoans (Calvet, 1900; Zimmer and Woollacott, 1977a). Several studies have designated two main larval axes in bryozoan larvae: the anterior–posterior and the aboral–oral axes (Fig. 1A–D). The aboral–oral axis is specified by the animal–vegetal axis of cleavage stages, and the anterior–posterior axis is largely marked by the positions of the pyriform complex, mouth, and anus (Zimmer, 1997). However, since much of the variation documented here correlates with the functional demands of dispersal and habitat exploration, I have chosen to emphasize the forward and aft regions of the larva during swimming and crawling behaviors.

Both feeding and nonfeeding bryozoan larvae possess a variety of surface cells that contribute to different ciliary fields, some of which have more than one function (Reed et al., 1988). Larval forms depicted in Figure 1 represent a few of the better-known species of marine bryozoans (Reed and

Woollacott, 1982; Stricker et al., 1988a,b; Zimmer and Woollacott, 1993; Santagata and Zimmer, 2000). Although there is more diversity in larval anatomy than depicted in Figure 1, it is useful when comparing the structure of the major ciliary fields to disregard the details of some larval sensory structures such as the ciliated ray cells, ocelli, and components of the pyriform organ (see Woollacott and Zimmer, 1972; Reed, 1988; Zimmer and Woollacott, 1989b). In general, the larval ciliary fields include an apical disc (AD, Fig. 1A), an anterior pyriform complex (PO, Fig. 1A), and a few minor cell groups (intercoronal cells, supracoronals cells, etc.), but the largest multiciliated cells comprise the coronal (C, Fig. 1A) and oral ciliated (OC, Fig. 1A) cellular fields. The relative proportions of the coronal and OC cellular fields vary among species. Together, the ciliary beat produced by these cellular fields can have similar or different roles in propelling the larva during swimming and crawling behaviors. Larval tissues differ from the presumptive juvenile tissues such as internal sac (IS) and pallial epithelium (PE), which consist of unciliated and largely undifferentiated cell types having no role in larval behavior. In several species, both PE and IS form the external body wall (cystid) of the ancestrula at metamorphosis (PE and IS, Fig. 1A–D). However, there are some differences among species and, where either the PE or IS does not contribute to the cystid; these structures are uncolored in Figure 1.

Figure 1A is based on the larval morphology of *Membranipora membranacea* (Stricker et al., 1988a,b) in which the numerous ciliated cells responsible for propelling the larva, the coronal cells (C, Fig. 1A), are positioned in a narrow band at the oral (aft) end of the larva. As with all marine bryozoan larvae, this form swims while rotating about a central axis with the AD (Fig. 1A) pointed forward. However, once contacting a suitable substratum, competent cyphonautes larvae explore the substrate propelled by the ciliary beat of the coronal cells and the ciliary tuft of the vibratile plume (VP, Fig. 1A). Relative to the position of the AD there is a 90° difference in the orientation of the larva during swimming and crawling behaviors. Some other features specific to the cyphonautes form are its triangular shape, bivalved shell (CS, Fig. 1A), the thin PE layer (PE, Fig. 1A), and the ciliated ridges (CRs) as well as other ciliated cells of the vestibule that bring food particles to the mouth (CR and VC, Fig. 1A).

Among the nonfeeding larval types, some of the most recognized are the coronate types of ascophoran cheilostome bryozoans such as *Schizoporella* (Reed, 1991) and *Watersipora* (Zimmer and Woollacott, 1989a). Among some coronate forms, the coronal cell region consists of 30 or 32 cells in a median transverse band that varies in surface area relative to the larval body size. One example of a coronate form like this is found in *Celleporaria brunnea* depicted in Figure 1B, in which the coronal cell field (C, Fig. 1B) covers about two thirds of the larval surface area, and the large flattened OC cells (Fig. 1B) are used mainly during crawling behaviors. The orientation of the larva during swimming and crawling behaviors is similar to that of *Membranipora*. In Figure 1B, the OC cells of *Celleporaria* are colored the same as the cells of the CRs and other ciliated cells present in the vestibule of cyphonautes larvae, because it is likely that a subset of these cell types are homologous. As with most other nonfeeding bryozoan larvae, the PE is invaginated and positioned around the AD (Fig. 1B).

Buguliform larvae such as those of *Bugula neritina* may be elongate in the aboral–oral axis or nearly spherical, and do not exhibit any significant difference in orientation of the AD during swimming and crawling behaviors (Woollacott and Zimmer, 1971). In *Bugula neritina* larvae, the coronal field is comprised of hundreds of cells (C, Fig. 1C); however, other species of *Bugula* have only 32 coronal cells as observed in most coronate forms (Reed et al., 1988). The OC cell field (Fig. 1C) is restricted to a narrow region around the oral pole of the larva and likely has little role in larval propulsion. In contrast to species such as *Celleporaria* or *Schizoporella*, the relatively small PE in *Bugula neritina* larvae does not contribute to the cystid at metamorphosis (PE, Fig. 1C).

Larval forms of ctenostome bryozoans from the family Vesiculariidae are strongly elongate in the aboral–oral axis (Reed and Cloney, 1982a), do not exhibit any significant difference in orientation of the AD during swimming and crawling behaviors, and the coronal cell field covers most of the larval surface (C, Fig. 1D). The field of OC cells (Fig. 1D) in vesiculariforms is comparatively smaller than that of most coronate forms, although it still contributes to crawling behaviors (Reed and Cloney, 1982b; Zimmer and Woollacott, 1993). Vesiculariform larvae have a comparatively large, asymmetrical PE (Fig. 1D) that forms all of the cystid at metamorphosis (Reed and Cloney, 1982b). In vesicularifoms such as *Amathia* and *Bowerbankia*, the IS (Fig. 1D) functions only in temporary attachment and is lost after metamorphosis (Reed, 1984; Zimmer and Woollacott, 1993).

One other difference in the structure of these larval forms is the arrangement of undifferentiated cell types that form the polypide at metamorphosis. Cell types believed to form the polypide at metamorphosis are shaded yellow in Figure 1 (UC, Fig. 1A–D), and this figure depicts most but not all the variation in position documented for these cell types within bryozoan larvae. At metamorphosis, the main morphogenetic movements that form the preancestrula are the eversion of the IS, the retraction of the apical disc, and the involution of the ciliated corona. These tissue rearrangements

leave components of the cystid on the outside and undifferentiated cells that will form the polypide as well the transient larval tissues on the inside of the preancestrula (for review, see Reed, 1991). Although there are some exceptions among species, the eversion of the IS and retraction of the AD are usually achieved through muscle-mediated morphogenetic movements (Reed, 1984; Stricker, 1988). Coronal cell involution and associated movements of the PE are more complex involving dynamic microfilaments, and possibly the reversal of coronal ciliary beat (Reed and Cloney, 1982b; Reed and Woollacott, 1982).

Considering the differences observed in anatomy among the few well-described larval forms of gymnolaemate and cyclostomate bryozoans, one question is how well the arrangements of larval ciliary fields and musculature of more diverse forms correlate with systematic groupings that are based largely on the characters of adult zooids. It is not surprising that there should be anatomical differences between feeding and nonfeeding larval types; however, the functional demands of active settlement behaviors and metamorphosis may result in both convergent and divergent larval anatomies. Overall, greater taxonomic sampling and detailed analysis of larval tissues are required to evaluate whether trends in larval anatomy follow systematic groupings or are influenced more by functional demands.

The purpose of this study was to gather detailed information on the ciliary fields and musculature among the larvae of the major morphological grades of marine bryozoans using confocal imaging techniques. Sampling effort focused on lesser-known species from genera with few published larval accounts. Since the structure of larval musculature has been described only from traditional histological and ultrastructural methods, several well-known species were reevaluated. The rich histological and ultrastructural information available from previously described species also served as an internal control for the data gathered through confocal microscopy. Taken together, the previously published information and confocal reconstructions presented here allowed greater three-dimensional resolution of the diversity of ciliary fields and musculature among the larvae of marine bryozoans. Overall, these results show that there is a congruence between larval and adult characters within select systematic groups of marine bryozoans; however; there is much more diversity in the structure of larval ciliary fields and musculature than previously documented, especially among nonfeeding ctenostome larval types. This structural diversification reflects differences in orientation of the AD during swimming and crawling behaviors, maximizing the surface area of cells with propulsive cilia, larvae that are elongate in the aboral–oral axis, and simplification of ciliary fields and musculature likely due to evolutionary loss.

MATERIALS AND METHODS

Collection of Animals

Adult colonies of *Crisia elongata* (Milne-Edwards, 1838), *Nolella stipata* (Gosse, 1855), *Amathia vidovici* (Heller, 1867), *Bugula stolonifera* (Ryland, 1960), *Bugula neritina* (Linnaeus, 1758), *Celleporaria sherryae* (Winston, 2005), and *Schizoporella floridana* (Osburn, 1914) were collected between 2002 and 2004 within the Indian River Lagoon, Florida. *Sundanella sibogae* (Harmer, 1915) and *Aeverrillia setigera* (Hinks, 1887) were collected at Sea Horse Key, Florida. Colonies were identified and kept in a dark incubator at 23°C and aerated for a few days at the Smithsonian Marine Station, Fort Pierce, Florida. These colonies were then exposed to light and released their brooded larvae. Late larval stages of *Membranipora membranacea* (Linnaeus, 1767) were collected from the plankton near the dock at Friday Harbor Laboratories, Friday Harbor, Washington, during April 2005.

Microscopy

Light micrographs were taken of live larvae crawling on glass slides with a Leica DMLB microscope, using a polarizing filter with a Nikon Coolpix 995 Camera. For staining of cell borders and musculature, larvae were anesthetized in filtered seawater and 7.5% magnesium chloride (mixed 2:1) for 20 min prior to fixation. Specimens were fixed overnight at 4°C in a 4% paraformaldehyde solution in 0.1 M Sorenson's phosphate buffer (pH = 7.4). Larvae were removed from this solution and larval tissues were permeablized with 0.1 M Sorenson's phosphate buffer and 0.1%–0.3% Triton-X detergent for 24 h at 4°C before proceeding with the staining protocol. All further steps were carried out on a rotary shaker table. Fibrous actin was stained with a 1:20 dilution of AlexaFluor 488 Phalloidin (A12379, Invitrogen-Molecular Probes) for 1 h. Stained larvae were adhered to clean glass slides coated with a poly-L-lysine solution (1:10 dilution, 25988-63-0, Sigma-Aldrich) and put through an alcohol dehydration series using 2-propanol within 4 min. Finally, larvae were cleared in a solution of benzyl benzoate and benzyl alcohol (2:1) for 2 min and mounted in the same solution. Slides were kept in the dark at 4°C until viewed with a BioRad Radiance 2100 laser confocal system and a Nikon E800 microscope. Confocal z-series were gathered with 1-μm sections. Volume renderings, surface renderings, and depth-coded z-projections were made with Voxx version 2 (Indiana University School of Medicine) and LSM image browser (Leica).

Specimens for scanning electron microscopy were prepared according to the methods of Reed et al. (1988). Fixed specimens for SEM were mounted on stubs with double-stick tape, then critical point dried and sputter-coated with gold–palladium. Larvae were examined with a JEOL JSM 6400V, and digital images were saved directly as TIFF files.

RESULTS

Current higher systematic groupings for bryozoans above the level of genus are often different depending on the author. This is particularly true of the ctenostome bryozoans (Jebram, 1992; Todd, 2000). What have been traditionally referred to as the carnose or stoloniferous ctenostome bryozoans may not be natural groupings, and the organization of families within superfamily assemblages are often dependent on the interpretation given to a few zooidal characters. For the purpose of this paper, I will retain *Nolella stipata*, *Sundanella sibogae*, and *Tanganella muelleri* under the superfamily Victorelloidea. Since many structures and cell types for

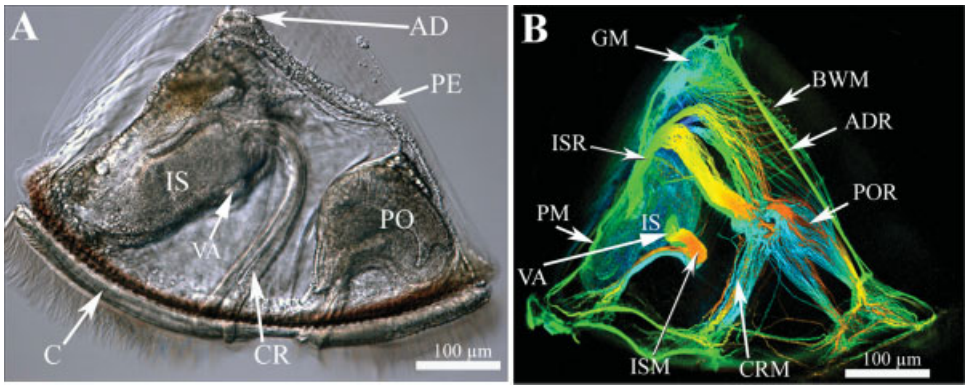

Fig. 2. Larval anatomy and musculature of *Membranipora membranacea*. **A:** Light micrograph of the cyphonautes larva of *M. membranacea* showing the main larval structures such as the apical disc (AD), pyriform organ (PO), coronal cells (C), ciliated ridges (CR), internal sac (IS), and pallial epithelium (PE). **B:** Depth-coded z-projection of a lateral view of a competent *M. membranacea* larva stained with phalloidin showing the musculature. The largest muscles are the paired retractors that insert on the internal sac (ISM and ISR) and are also associated with the valve adductor muscle (VA). There are also several sets of muscles with striated fibers such as the muscles below the ciliated ridges (CRM), circular muscle fibers surrounding the gut (GM), paired retractor muscles of the pyriform organ (POR), the apical disc retractor (ADR), the posterior medial muscle (PM), and circular muscles of the body wall (BWM).

bryozoan larvae have been originally described from cheilostome bryozoans, it is simplest to begin with these forms. Where information on larval anatomy was published previously for some species (such as *Membranipora*, *Bugula*, and *Amathia*), details of ciliated cell types are reviewed briefly.

Class Gymnolaemata: Order Cheilostomatida

Membranipora membranacea (superfamily Membraniporoidea): Feeding cyphonautes larva. Late stage larvae of *Membranipora membranacea* are shaped similar to a blunt-ended triangle covered in a bivalved shell and commonly referred to as a cyphonautes larva (Fig. 2A). The coronal cells (C, Fig. 2A) are restricted to a thin band of numerous ciliated cells at the oral (aft) end of the larva. This larval form feeds on plankton by filtering particles out of the surrounding water via ciliary beat. Anatomical features unique to feeding bryozoan larvae are the CRs (Fig. 2A) and other ciliated cells of the vestibule that bring food particles to the mouth and gut. Larval structures present in *M. membranacea* that are also found in nonfeeding forms are the pyriform organ (PO), IS, and AD (Fig. 2A).

Musculature in the larva of this species is extensive, consisting of circular muscles of the body wall and gut as well as retractors of the IS, AD, and pyriform complex (Fig. 2B). The largest muscles are the paired sets of smooth muscles that insert on opposite sides of the midpoint of the internal sac (ISR and ISM, Fig. 2B). These muscles differ in their origins. The internal sac retractors (ISR) originate from a central position within the larval body. The more orally positioned pair of internal sac muscles (ISM, Fig. 2B) form a checkmark shape and originate from less dense fibers near the coronal cells at the posterior pole of the larva. The ISMs are also connected to the valve adductor muscle (AM, Fig. 2B) that is positioned at the midpoint of the IS on its oral side. Together the valve adductor muscle (VA) and the paired ISMs have a "chair-like" shape. Numerous layers of striated muscle fibers underlie the CRs (CRM, Fig. 2B). The gut tissue has a series of circular muscle fibers along its length (GM, Fig. 2B). A pair of striated retractor muscles originates centrally in the larval body and insert on lateral sides of the pyriform organ (POR, Fig. 2B). Striated circular muscles of the body wall are found in the aboral portion of the larva (BWM, Fig. 2B). Two longitudinal striated muscles that underlie the PE originate from the AD near a centrally located myoepithelial cell and insert on opposite ends of the oral side of the larva (ADR and PM, Fig. 2B). The apical disc retractor (ADR) inserts on the pyriform organ and the posterior medial muscle (PM) connects with muscle fibers that underlie the coronal cells near the posterior side of the larva.

Celleporaria sherryae (superfamily Lepralielloidea): Nonfeeding coronate larva. Adult colonies of *Celleporaria sherryae* release orange-pigmented coronate larvae that are ~170 µm in diameter. Once released, these larvae swim in a circle as they are initially tethered to the maternal zooid by a mucous cord that is connected at the glandular field of the pyriform organ. Scanning electron micrographs show most of the larval surface to be covered with multiciliated cells divided into three main regions (Fig. 3A). Two thirds of the larval surface area is covered by cilia of coronal cells extending above and below the equatorial region (CC, Fig. 3A). There is also a clear bound-

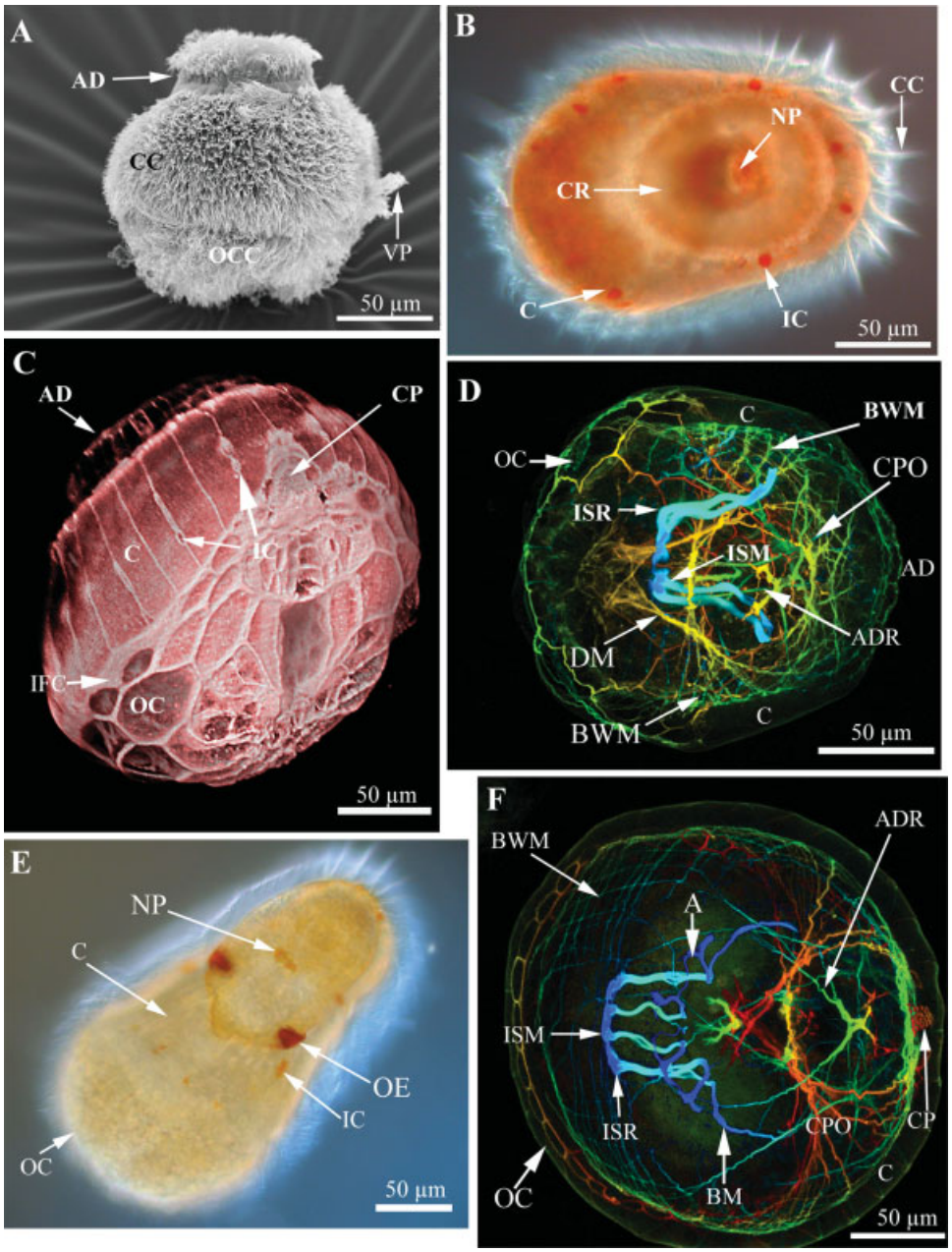

Fig. 3. Larval anatomy and musculature of *Celleporaria sherryae* and *Schizoporella floridana*. **A:** SEM of a lateral view of the coronate larva of *C. sherryae* showing the apical disc (AD), coronal cell cilia (CC), cilia of the oral cells (OCC), and bundles of cilia of the vibratile plume cells (VP). **B:** Light micrograph looking down on the apical disc of larva of *C. sherryae* showing several of the pigmented intercoronal cells (IC) positioned between adjacent coronal cells. The apical disc is mainly composed of radially arranged ciliated ray cells (CR) and an inner group of neuronal plate cells (NP). **C:** Cell surface projection of the larva of *C. sherryae* showing the strap-like coronal cells (C) and oral ciliated cells (OC). The borders of intercoronal cells (IC) are prominent between the first and second pairs of coronal cells. Other notable groups of cells include the ciliated plaque cells (CP) positioned within the pyriform complex and the undifferentiated infracoronal cells (IFC) positioned between the coronal and oral ciliated cell fields. **D:** Depth-coded z-projection of a lateral view of the musculature of *C. sherryae*. The musculature consists of large paired retractors (ISM and ISR), diagonal muscles (DM), small apical disc retractors (ADR), crisscrossing musculature of the pyriform complex (CPO), and orthogonal muscle fibers in the body wall (BWM). **E:** Light micrograph looking down on the apical disc of the coronate larva of *S. floridana* showing the pigmented cups of the posterolateral ocelli (OE), some pigmented intercoronal cells (IC), neural plate cells (NP), and coronal cells (C). **F:** A depth-coded z-projection of the musculature of *S. floridana* looking down on the apical disc. The paired retractors (ISM and ISR) have specialized anchors (A) posterior to the apical disc, and the outer pair of retractors (ISR) also have extensions that border the apical disc on lateral sides (BM). Crisscrossing muscles in the pyriform complex (CPO) and orthogonal fibers in the body wall (BW) are also evident.

ary between the cilia of coronal cells and the cilia of the OC cells situated on the oral side of the larva (OCC, Fig. 3A). Like other bryozoan larvae, this species swims leading with the AD (Fig. 3A) while spinning about a central axis. While swimming these larvae are spheroid-shaped; however, they often assume a blunt-ended teardrop shape when crawling over a substrate (Fig. 3B).

Celleporaria sherryae larvae have at least five bilaterally symmetrical pairs of red-pigmented intercoronal cells (IC, Fig. 3B) positioned between particular adjacent pairs of coronal cells. No attempt was made to document the total number of ICs at each position. However, ICs are visible at position 1|1 (between the first pair of coronal cells counting from the anterior midline), 1|2, 3|4, 5|6, 7|8, 10|11, and 13|14 (Fig. 3B). Neuronal cells positioned in the middle of the AD (neural plate cells, NP, Fig. 3B) also share this red pigment. Cell surface staining with phalloidin revealed cell borders and clearly delineated the rectangular morphology of the 30 coronal cells and the positions of several ICs (C and IC, Fig. 3C). OC cells are irregularly shaped and have cell borders that stain prominently for fibrous actin (OC, Fig. 3C). The pyriform organ consists of the superior and inferior glandular fields, ciliated plaque, VP cells, the ciliated groove (CG), and specialized cells that border this groove.

Figure 3D is composed of transverse sections through the larva (from the aboral to the oral side) viewing musculature beneath the coronal cell layer. Musculature in the larvae of *Celleporaria sherryae* includes an orthogonal framework of body wall muscle fibers (BWM, Fig. 3D), diagonal muscles of the body wall associated with the internal sac (DM, Fig. 3D), and the large curved retractors (ISM and ISR, Fig. 3D). The latter muscles originate beneath the base of the AD adjacent to the IS. The overall shape of these muscles would be similar to a horse-shoe that had its tips bent in opposite directions.

Schizoporella floridana (superfamily Schizoporelloidea): Nonfeeding coronate larva. Adult reproductive colonies of *Schizoporella floridana* are often found growing on blades of *Thalassia testudinum* during winter (January) in the Indian River Lagoon. Larvae are pigmented a light orange and have a pair of conspicuous posterolateral ocelli located above the corona and a single anteromedial ocellus between the first pair of coronal cells. All of these ocelli have red-pigmented cups (OE, Fig. 3E). The pigmented cups of the posterolateral ocelli are composed of supracoronal cells, but the pigment cup of the anteromedial ocellus is a modification of the two adjacent coronal cells (not figured). The neural plate cells and several small, inconspicuous ICs also have the same red pigment at their apex (NP, Fig. 3E). *Schizoporella floridana* larvae consistently have 32 coronal cells as well as a band of supracoronal cells. Overall, the coronal and OC cellular fields of *S. floridana* are slightly expanded as compared to those of *Celleporaria sherryae*.

Figure 3F is composed of frontal sections through the AD progressing downward toward the oral side of the larva. Musculature of this species is much like that of *Celleporaria*. The largest muscles are the paired retractors associated with the IS and AD (ISM and ISR, Fig. 3F). These large, curved retractors have similar origin and insertion points to the corresponding muscles in *Celleporaria*. However, in *Schizoporella floridana* the outer pair of retractors has a modified split anchor-like end (A, Fig. 3F), and there is also a muscle that borders the right and left sides of the AD (BM, Fig. 3F). An orthogonal layer of body wall musculature is also present (BWM, Fig. 3F). Crossing muscle fibers are numerous in the anterior half of the larva (MF, Fig. 3F). Cell borders are always visible, but those of the ciliated plaque and OC cells stained more heavily for fibrous actin (OC and CO, Fig. 3F) than other cell types. Similar to larvae of *Celleporaria*, *Schizoporella* larvae have a dense network of diagonal muscle fibers near the pyriform complex (MP, Fig. 3F) and also have longitudinal muscles that border the CG.

Bugula spp. (superfamily Buguloidea): Nonfeeding buguliform larvae. The larvae of *Bugula stolonifera* are spheroid-shaped and ~120–150 μm in diameter. This species has a pair of posterolateral ocelli (OE, Fig. 4A) as well as a pair of anteromedial ocelli near the large fused ciliary tufts of the VP (Fig. 4A). Larvae have 32 cuboidal coronal cells that cover the majority of the larval surface area (CC, Fig. 4A). Although present, the OC cell region is reduced within buguliform larvae. Muscles within *B. stolonifera* larvae are limited to bilaterally symmetrical sets of crossing axial muscles (AM, Fig. 4B) between the AD and the IS as well as muscles that are positioned between lateral sides of the larval body. Beneath the coronal cell layer is an orthogonal grid of BWM fibers (Fig. 4B).

Larvae of *Bugula neritina* are large (sometimes elongate) spheroids ~300–500 μm in diameter and have two conspicuous posterolateral ocelli with darkly pigmented surrounding cells (OE, Fig. 4C). *Bugula neritina* larvae have several hundred coronal cells over their surface, but only six distinctly pigmented regions beneath the larval corona where ICs are positioned along the larval equator (IC, Fig. 4C). Musculature is less developed than in other species. Besides the orthogonal meshwork of body wall musculature (BWM, Fig. 4D), the only other significant muscles are the axial muscles positioned between the AD and IS (ADR, Fig. 4D). Although not shown in Figure 4B,D, both species of *Bugula* have longitudinal muscles bordering the CG.

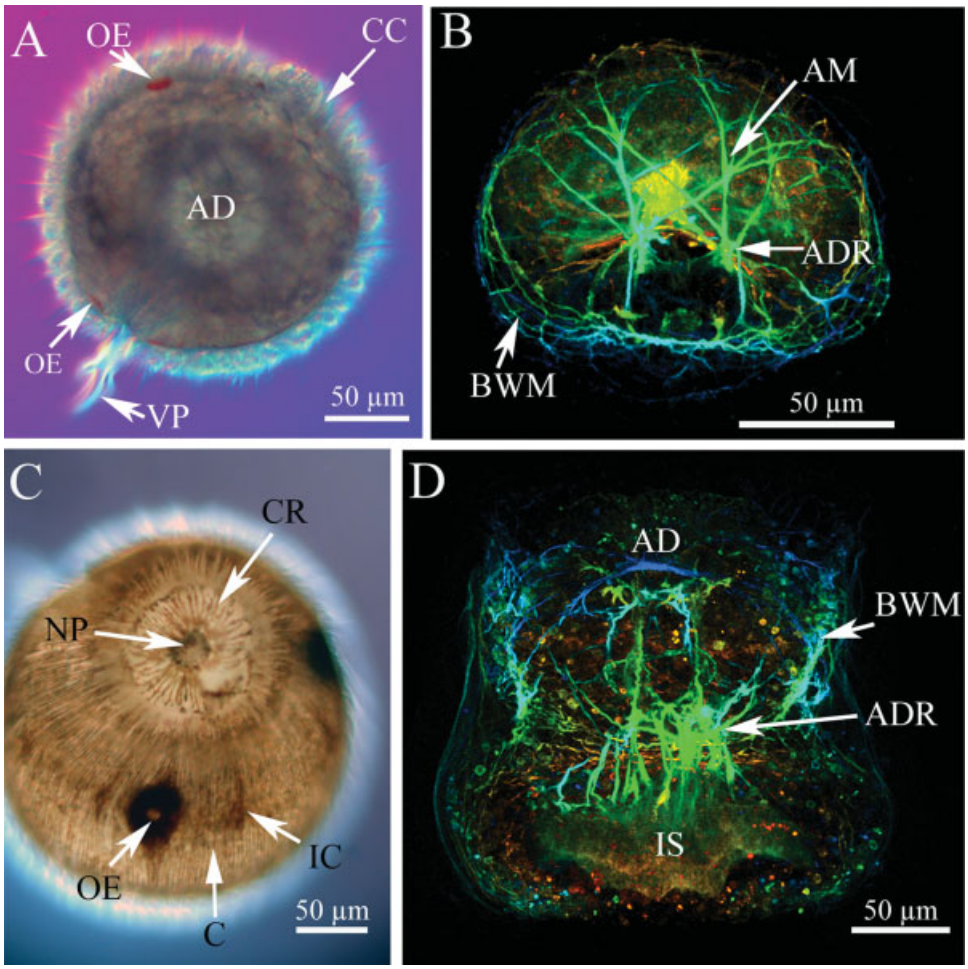

Fig. 4. Larval anatomy and musculature of *Bugula stolonifera* and *Bugula neritina*. **A:** Light micrograph looking down on the apical disc (AD) of the buguliform larva of *B. stolonifera* showing the ciliary bundles of the vibratile plume (VP), cilia of the coronal cells (CC), and the paired anterolateral and posterolateral ocelli (OE). **B:** A depth-coded z-projection of the musculature of *B. stolonifera* looking down on the apical disc. The more simplified musculature of this species consists of the axial muscles (AM), the apical disc retractors (ADR), and the orthogonal muscle fibers within the body wall (BW). **C:** Light micrograph of the buguliform larva of *B. neritina* showing the numerous coronal cells (C), large posterolateral ocelli (OE), intercoronal cells (IC), ciliated ray cells (CR), and neural plate cells (NP). **D:** Depth-coded z-projection of a lateral view of the musculature of *B. neritina* showing the retractor muscles (ADR) positioned between the apical disc (AD) and internal sac (IS) as well as the muscle fibers of the body wall (BWM).

Class Gymnolaemata: Order Ctenostomatida

Sundanella sibogae (superfamily Victorelloidea): Nonfeeding larva. The larva of *Sundanella sibogae* is a relatively large cylindrical form often 0.8–1.0 mm in length that is elongate in the aboral–oral axis and has a relatively wide apical

Fig. 5. Larval anatomy and musculature of select species of ctenostome and cyclostome bryozoans. **A:** Depth-coded z-projection of a lateral view of the larva of *Sundanella sibogae* showing the numerous multiciliated coronal cells (C) and oral ciliated cells (OC). Musculature of this species includes at least three pairs of large retractor muscles (ISM and ISR) positioned near the larval equator. **B:** Close-up and oral view of the cellular anatomy and musculature of *S. sibogae* showing the longitudinal muscles that line the body wall (BW), the relatively large ciliated groove (CG), and retractor muscles (ISM and ISR). **C:** Light micrograph of a lateral view of the larva of *Nolella stipata* (ctenostome bryozoan) showing the small apical disc (AD), simple internal sac (IS), and the pigmented band (P) of cells positioned along the larval equator. Cells with small ciliated tufts (CT) are evident within the pigmented cell region. **D:** Depth-coded z-projection of the larval musculature of *N. stipata* showing the cells with ciliated tufts (CTC) and the borders between the numerous multiciliated cells (MC) that cover most of the larval surface. Musculature consists of simple apical disc retractors (ADR) and muscle fibers that border the small ciliated groove (CGM). F-actin staining is also more evident at the apices of the pallial epithelium cells (PE) near the apical disc (AD). **E,F:** Depth-coded z-projections of posterior and anterior views of the musculature of the vesiculariform larva of *Amathia vidovici* (ctenostome bryozoan). This species has simple circular muscles in the aboral (AM) and equatorial (EM) regions as well as a small apical disc (AD) with neural plate (NP) and ciliated ray cells (CR). Longitudinal muscles (CGM) border the ciliated groove. **G:** Light micrograph of a lateral view of the larva of *Aeverrillia setigera* (ctenostome bryozoan) showing the darkly pigmented coronal cells (C), apical disc with ciliated ray (CR) and neuronal plate cells (NP), and the large ciliated groove (CG). **H:** SEM of *A. setigera* showing the portions of the larval surface covered by the coronal cells versus the oral ciliated cells. **I,J:** Depth-coded z-projections of the cell borders and musculature of *A. setigera*. The apical disc (AD) is comparatively small compared to the wide surrounding region of the invaginated pallial epithelium (PE). Sixty-four coronal cells (C) cover about a third of the total larval surface area at the aboral end of the larva. There is a single band of ciliated cells (CTC) between the large coronal and oral ciliated cell (OC) fields. The ciliated groove (CG) is large and bordered by two longitudinal muscles (CGM). A series of longitudinal retractors (ADR) originate on the apical disc and insert on the lateral borders of the ciliated groove. **K:** Depth-coded z-projection of the larval musculature of *Crisia elongata* (cyclostome bryozoan). Musculature of this species is comprised solely of simple longitudinal muscle fibers (MF). Numerous hexagonal multiciliated cells (MC) cover the surface of the larva.

region (Fig. 5A). The cell borders of the multiciliated cells in the oral half of the larva stain heavily for fibrous actin much like the OC cells of cheilostome forms. Furthermore, the multiciliated cells in the aboral half of the larva do not stain heavily for fibrous actin, consistent with the features of coronal cells from other forms. Therefore, I have labeled these cells as coronal (C) and OC cells (OC) in Figure 5A.

The majority of the musculature of this species consists of large sets of retractors positioned centrally within the larva (ISM and ISR, Fig. 5A, B). Although the proximity and morphology of these muscles makes it difficult to discern their exact number, there are at least three distinct pairs (perhaps four) of retractors. The anchor points for these muscles are located centrally on the oral side of the larva, where each muscle converges toward

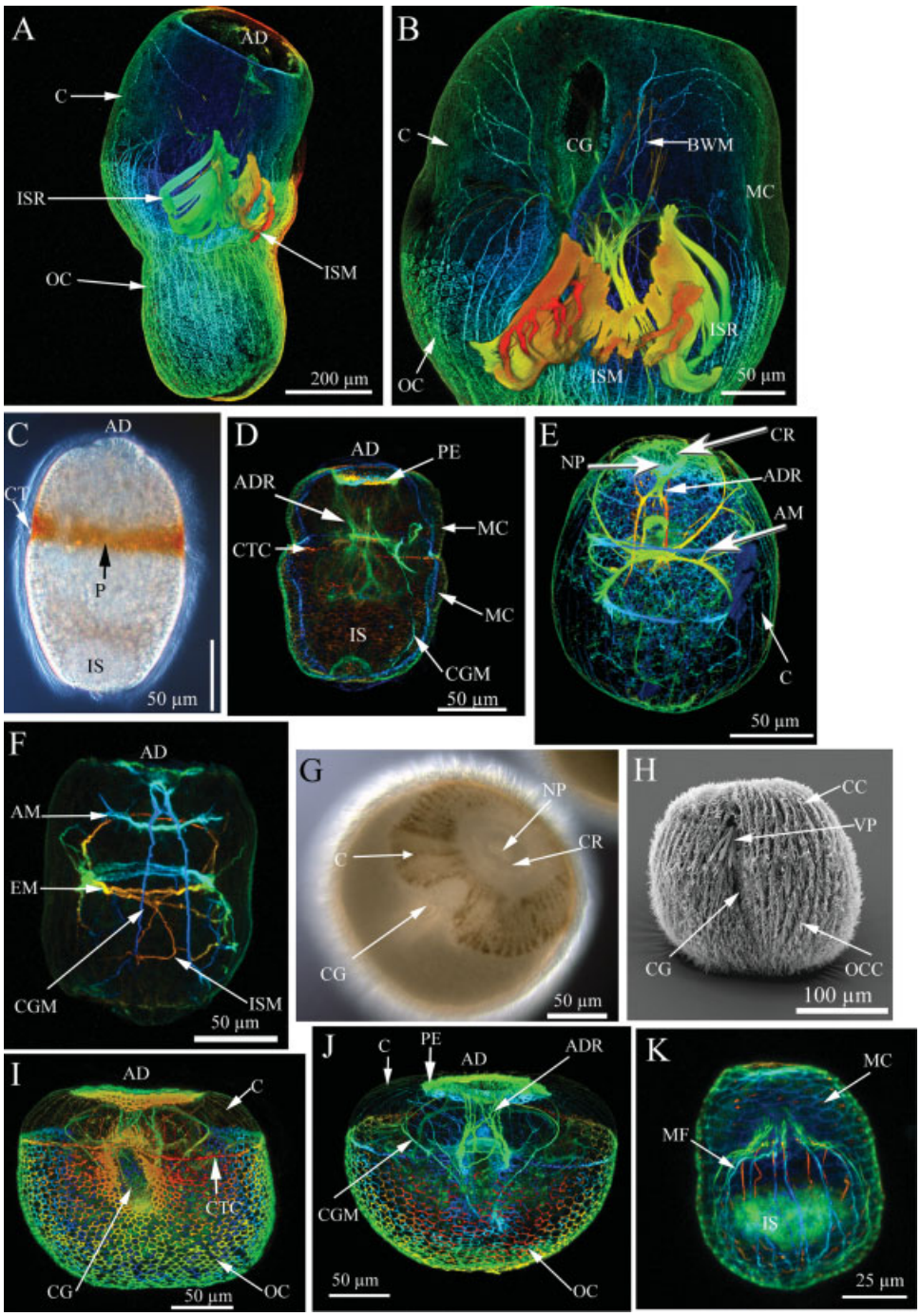

Figure 5.

the larval midline near the CG (Fig. 5B). This larva also has several longitudinal muscles within the body wall that are positioned in parallel paths along the length of the body (BWM, Fig. 5B).

Nollela stipata (superfamily: Victorelloidea): Nonfeeding larva. This species is elongate in the aboral–oral axis and slightly compressed in the anterior–posterior axis. There is no distinct CG in this species, and only a small ciliated pit. The larva has a relatively small AD and an equatorial band of pigmented cells (P, Fig. 5C). Within the band of pigmented cells are cells with small ciliary tufts (CT, Fig. 5C) that are arranged radially around the circumference of the larva. The larval surface is covered by multiciliated cells (Fig. 5C) that stain uniformly for fibrous actin in both the aboral and oral halves of the larva (MC, Fig. 5D). Because of this uniform staining of F-actin, there are no cell groups that can be specifically labeled as coronal or OC cells. However, a clear demarcation between the aboral and oral halves of the larva is defined by the cell borders of the ciliary tuft cells (CTC, Fig. 5D). These CTCs are similar in morphology to other sensory cell types (ICs) found in larvae from other bryozoan species.

Musculature for this species is minimal. In comparison with other species there are relatively few muscle fibers within ADRs (Fig. 5D). The only other distinct muscle in this species is a longitudinal muscle that is positioned along the length of the larva bordering the ciliated pit (CGM, Fig. 5D). The apices of the PE cells near the AD also stain heavily for fibrous actin (PE, Fig. 5D).

Amathia vidovici (superfamily Vesicularioidea): Nonfeeding vesicullariform larva. Vesiculariform larvae are elongate in the aboral–oral axis and have a comparatively small AD (Fig. 5E). Phalloidin also stains fibrous actin in the cell borders of coronal cells and OC cells differently within this species. Approximately 40 wedge-shaped coronal cells cover most of the larval body (C, Fig. 5E). ICs are positioned between adjacent coronal cells in the aboral, equatorial, and oral regions of the larva. The OC cells are flattened and cover a restricted area of the oral region of the larva adjacent to the opening of the IS.

The major muscles of the larval body within *Amathia vidovici* are the equatorial and aboral ring muscles (EM and AM, Fig. 5E,F), the longitudinal muscle fibers that border the CG (CGM, Fig. 5F), and the relatively short AD retractors that insert on the pyriform organ (ADR, Fig. 5E,F). There is also a network of muscle fibers connecting the equatorial ring muscle with the IS (ISM, Fig. 5F).

Aeverrillia setigera (superfamily Aeverrillioidea): Nonfeeding larva. Larvae of *Aeverrillia setigera* are elongate in the aboral–oral axis and compressed in the anterior–posterior axis (Fig. 5G). This species is cream-colored, except for the coronal cells that have brown pigment granules (C, Fig. 5G). The CG (CG, Fig. 5G) is relatively large in this species, but similar to *Amathia*, the AD is relatively small (AD, Fig. 5G). In scanning electron micrographs, the dense ciliation of the coronal cells (CC, Fig. 5H) and the bundles of fused cilia of the VP (Fig. 5H) are evident. In contrast to vesiculariform larvae (but similar to *Sundanella*), the OC region is expansive, and its cilia beat metachronally in coordination with the ciliary beat of the coronal cells (OCC and CC, Fig. 5H).

Cell borders of coronal cells and OC cells have the same staining characteristics as found in most other nonfeeding gymnolaemate larval forms. There are 64 coronal cells and numerous OC cells (C and OC, Fig. 5I). The coronal and OC cell regions of the larva are separated by a band of small ciliated sensory cells similar to those observed in *Nolella* (CTC, Fig. 5I). The apices of the pallial epithelial cells that border the AD also stain heavily for fibrous actin (PE, Fig. 5I,J). Musculature consists primarily of the ADRs that insert near the equatorial region of the larva on the oral side (ADR, Fig. 5J). The only other muscles are the longitudinal muscles bordering the CG (CGM, Fig. 5J); these are bowed more laterally in this species than in other larval forms.

Class Stenolaemata: Order Cyclostomata

Crisia elongata (family Crisinidae): Nonfeeding larva. Larvae of *Crisia elongata* lack an AD and have numerous hexagonal-shaped multiciliated cells that cover the entire surface of the spheroid-shaped larva. The cell borders of these cells stained uniformly for fibrous actin. There is no difference in the morphology of the multiciliated cells in either the aboral or oral halves of the larva (MC, Fig. 5K). As a consequence of this cellular uniformity, there are no cell groups that can be specifically labeled as coronal or OC cells. Muscular anatomy is comprised of ~20 thin muscle fibers (MF, Fig. 5K) that originate from the middle of the base of the PE near of the forward end of the larva and travel aft around the IS (IS, Fig. 5K).

DISCUSSION

Arrangement of the Main Ciliary Fields

The cellular arrangement, position, and degree to which the main propulsive ciliary fields cover the surface of bryozoan larvae are clearly mutable characters. Considering the origins of the cyclostome, ctenostome, and cheilostome bryozoans in the fossil record (Taylor, 1990; Lidgard et al., 1993), zooidal characters (Todd, 2000), and some molecular phylogenetic evidence (Dick et al., 2000), the pleisiomorphic condition for larval traits (at least for extant forms) may be similar to the condition found in larval forms present within the genus *Alcyonidium*. This genus includes species having either feeding

TABLE 1. Select larval traits across the morphological grades of marine bryozoans

Species	Order/larval type/larval shape	Coronal and oral ciliated cells	Swim–crawl orientation	Musculature
Crisia elongata	Cyclostomata/nonfeeding **Cylcoform**/spheroid	Type 1	Same	Simple LM
Alcyonidium albidum	Ctenostomatida/feeding Cyphonautes/laterally compressed pyramid	Type 2	90° difference	ADR, AM, ISM, ISR, VA, GM, CRM[a]
Alcyonidium gelatinosum[b]	Ctenostomatida/nonfeeding Coronate/spheroid compressed in the aboral–oral axis	Type 3	90° difference	ADR, ISM, ISR, CGM[c]
Flustrellidra hispida	Ctenostomatida/nonfeeding Psuedocyphonautes/ Pyramidal	Type 2	90° difference	ADR, PM, ISM?, ISR?[d]
Tanganella muelleri	Ctenostomatida/nonfeeding Coronate/spheroid compressed in the aboral–oral axis	Type 3	90° difference	ADR, EM, POR, ISM?, ISR?[e]
Nolella stipata	Ctenostomatida/nonfeeding **Nolelliform**/elongate in the aboral–oral axis	Type 1	Same	Simple ADR, CGM
Sundanella sibogae	Ctenostomatida/nonfeeding **Sundanelliform**/elongate in the Aboral-Oral Axis	Type 4	Same	ADR , ISM, ISR
Aeverrillia setigera	Ctenostomatida/nonfeeding **Aeverrilliform**/Elongate in the aboral–oral axis	Type 5	Same	ADR, CGM
Bowerbankia gracilis, Zoobotryon verticillatum, and *Amathia vidovici*	Ctenostomatida/nonfeeding Vesiculariform/elongate in the aboral–oral axis	Type 6	Same	Simple ADR, AM, EM, CGM[f]
Membranipora membranacea	Cheilostomatida/feeding Cyphonautes/laterally compressed pyramid	Type 2	90° difference	ADR, VA, ISM, ISR, POR, GM[g]
Celleporaria brunnea and *Celleporaria sherryae*	Cheilostomatida/nonfeeding Coronate/spheroid compressed in the aboral–oral axis	Type 3	90° difference	Simple ADR, ISM, ISR, POR, CGM[h]
Schizoporella floridana	Cheilostomatida/nonfeeding Coronate/spheroid compressed in the aboral–oral axis	Type 3	90° difference	ADR, ISM, ISR, POR, CGM
Bugula neritina and *Bugula stolonifera*	Cheilostomatida/nonfeeding Buguliform larva/elongate in the aboral–oral axis	Type 6	Same	ADR, CGM

Type 1: Coronal and oral ciliated cells not differentiated, uniform multiciliated cells present over larval surface. Type 2: Narrow band of numerous coronal cells positioned at the oral end of the larva. Type 3: Ring of 30 or 32 coronal cells positioned on the larval equator or covering more than half of the larval surface; oral ciliated cells flattened and modified for crawling. Type 4: Numerous coronal cells and oral ciliated cells dividing the larval body into aboral and oral halves; oral ciliated cells modified for swimming propulsion. Type 5: Sixty-four rectangular coronal cells in the aboral half of larva and numerous oral ciliated cells in oral half; oral ciliated cells modified for swimming propulsion. Type 6: Thirty-two to hundreds of elongate coronal cells that cover most of the larval surface, and a small field of oral ciliated cells that have a reduced role in propulsion. Larval types in bold text denote a new term proposed for a general larval type within a particular systematic group.

Abbreviations: apical disc retractor (ADR), aboral muscle (AM), ciliated groove muscle (CGM), ciliated ridge muscle (CRM), equatorial muscle (EM), gut musculature (GM), internal sac muscles (ISM), internal sac retractors (ISR), longitudinal muscles (LM), parietal muscles (PA), muscles of the pyriform organ (POR), and valve adductor muscle (VA).

References for larval anatomical data not presented in this paper.

[a]Prouho, 1892; [b]Larval type formerly attributed to *Alcyonidium polyoum*, Ryland and Porter, 2006; [c]d'Hondt, 1973; [d]Prouho, 1890; Zimmer and Woollacott, 1977a; [e]Zimmer and Reed, 1994; [f]Reed and Cloney, 1982a, Zimmer and Woollacott, 1993, Santagata, personal observations; [g]Stricker et al., 1988a; [h]Santagata and Zimmer, 2000; Question marks are placed next to muscle types where the level of detail was insufficient to determine their presence or absence from published reports.

cyphonautes larvae, nonfeeding psuedocyphonautes larvae, or nonfeeding coronate-like larval types (see Table 1). Regardless whether larval characters present in species of *Alcyonidium* or other basal ctenostome genera reflect the pleisiomorphic condition for extant bryozoans, the evolutionary modification

of feeding and swimming structures among the body plans of cyphonautes, pseudocyphonautes, and various nonfeeding bryozoan larval forms appears gradual or supportive of numerous combinations of anatomical traits (Table 1). This is particularly evident in evolutionary modifications of the propulsive ciliary fields. Functional dependence upon larval structures associated with the cyphonautes form such as the vestibule, CRs, gut, and the shell valves may limit morphological modifications to propulsive ciliary fields. The reduction, absence (possibly loss), or functional co-option of cyphonautes-specific characters is correlated with at least five different arrangements of the coronal and OC cellular fields (Table 1). The simplest ciliary propulsive fields are found in cyclostome larvae (data presented here and also in d'Hondt, 1977) and at least one species of ctenostome bryozoan (*Nolella stipata*). Considering the origin and evolutionary distance between cyclostome and ctenostome bryozoans (Lidgard et al., 1993), this similarity in form is likely due to convergent evolutionary loss.

The greater morphological complexity in the propulsive ciliary fields found in most nonfeeding larval forms of gymnolaemate bryozoans is linked to the orientation of the AD during larval swimming and crawling behaviors as well as larval shape. Coronate larva forms that are oriented similarly to cyphonautes larval types during swimming and crawling behaviors are present within the genus *Alcyonidium* (Zimmer and Woollacott, 1977a), *Tanganella* (Zimmer and Reed, 1994), and numerous cheilostome bryozoans. The coronal cells of these coronate larval types usually consist of a ring of 32 cuboidal-shaped cells. Nonfeeding coronate larvae of this type (here called Type 3, Table 1) also share in the morphology and function of the OC field that is used mainly during crawling behaviors. The remaining arrangements of the coronal and OC cell fields (Types 4–6) are all found in larval forms that are elongate in the aboral–oral (fore-aft) axis and also swim and crawl in the same orientation. These features are found in at least three different superfamilies within the ctenostome bryozoans (Victorelloidea, Aeverrillioidea, and Vesicularioidea) and at least one superfamily within the cheilostomes bryozoans (Buguloidea). Among these elongate nonfeeding larval forms, coronals cells number from 32 to hundreds and the coronal cell field can be restricted to the aboral half of the larva as in *Aeverrillia* or cover the majority of the larval surface as it does in vesiculariform and buguliform larval types. Having numerous OC cells with a ciliary beat mainly producing swimming propulsion is a feature shared by *Aeverrillia* and *Sundanella*. An elongate larval shape and expansion of the coronal cell layer are convergent features of both vesiculariform and buguliform larvae, especially when compared to the divergent morphology of their internal larval and presumptive juvenile tissues (Lyke et al., 1983; Zimmer and Woollacott, 1993). Overall, the repeated evolution of larval forms elongated in the aboral–oral axis may have preceded the diversification of the number and function of the cells within the coronal and oral fields. This functional diversification of ciliary fields within nonfeeding larval forms also corresponds with species radiations from the fossil record (Taylor, 1988). Developmentally, much of the variation in propulsive ciliary fields can be explained by the timing and number of cell divisions of coronal cell precursors (heterochrony) pre- and postgastrulation. Similar developmental modifications of cell divisions are also known from trochophore larvae of annelids and mollusks (Van den Biggelaar et al., 1997).

Larval Musculature

Besides the muscles responsible for retraction and extension of the pyriform organ, the musculature in bryozoan larvae plays important roles in maintaining larval shape and providing structural support. This is particularly evident in the cyphonautes type in which numerous striated muscles support the rigid pyramidal shape with several anchor points on the outer shell. Structural support is also added to the CRs, pyriform organ, and gut by a series of striated muscles.

Other than its structural and behavioral functions, larval musculature in bryozoans plays a significant role in eversion of the IS and retraction of the AD at metamorphosis (Reed and Woollacott, 1982; Reed, 1984; Stricker, 1988). In *Membranipora membranacea* larvae, lateral striated musculature causes the initial eversion of the IS (Stricker, 1988). Musculature described here largely supports this interpretation, but the greater detail revealed by confocal microscopy shows a second pair of muscles that insert on the oral side of the IS (ISR) in addition to the ISMs. Furthermore, this second set of ISRs is integrated with the valve adductor muscle. Together with the striated musculature of the CRs, pyriform retractors, and median muscles, this musculature everts and spreads the IS, and then flattens the preancestrula over the substrate.

Considering the presence of the large paired retractors in both feeding and nonfeeding larval forms of both ctenostomes and cheilostomes bryozoans, it is likely that the absence of these muscles in cyclostomes and some ctenostomes (*Nolella* and the family Vesiculariidae) is due to independent losses. The absence of the large retractor muscles and striated musculature in any known nonfeeding larval form suggests that these muscle types do not represent a functional constraint for morphogenetic movements at metamorphosis. Morphogenetic movements in some nonfeeding forms may be driven by microfilaments, and the heavy stain-

ing for fibrous actin in the PE of *Nolella* and *Aeverrillia* may be functionally linked to this process. This hypothesis is further supported by the modifications of the origin and insertion points for the large, paired retractor muscles in several nonfeeding larval forms (*Sundanella*, *Celleporaria*, and *Schizoporella*) as compared to their arrangement in feeding cyphonautes larvae.

One functional constraint regarding the usage of larval musculature at metamorphosis may involve axial or longitudinal muscles that internalize the undifferentiated cells that eventually form the polypide of the ancestrula. These cells are often positioned within or near the AD (or the aboral region of the larva in forms where the AD is absent such as *Crisia*, see d'Hondt, 1977) and are possibly located in the infracoronal region of some coronate larval types (Zimmer and Woollacott, 1989a; Santagata and Zimmer, 2000). Since the position and complexity of the AD and cells that form the polypide have been modified several times, muscle types and their arrangement have been modified as well. The only muscles present in several larval types with a simple arrangement of the polypide precursor cells are the axial muscles (ADRs or longitudinal muscles) positioned between the base of the AD and the roof of the IS (or the oral side of the larva). Conversely, elaboration of larval and presumptive juvenile tissues coincides with the presence of a more complex larval musculature. Across all morphological grades of larvae, structural complexity of musculature best correlates with two functional demands: 1) the position and structural complexity of the IS, and its eversion at metamorphosis, and 2) the position and complexity of cell types that form the polypide at metamorphosis.

Establishing any level of homology between the musculature of bryozoan larvae and the musculature of larval forms from other lophotrochozoan phyla is difficult. Among the lophophorates, clear comparisons can be made between the larval neuromuscular systems of brachiopods and phoronids (Santagata and Zimmer, 2002). However, feeding and nonfeeding bryozoan larval forms do not share any muscular characters with the larvae of phoronids or brachiopods. Among other lophotrochozoan larval forms, the shell retractors of larval gastropods (Page, 1998) bear some resemblance to the large paired retractors found in bryozoan larvae. Interestingly, retractors in larval gastropods are also associated with the shell gland that shares some functional similarity with the IS of bryozoan larvae. Whether these morphological and functional similarities are the result of an evolutionary conserved developmental program requires further research.

Larval Morphology and Phylogeny

Despite the diversity of cellular arrangements and musculature found in various types of bryozoan larvae, greater morphological conservation of larval tissues is present within each of the three orders of extant marine bryozoans than among these morphological grades that are based on adult zooidal traits. Among the ctenostome bryozoans, species within particular families such as the Vesiculariidae have clearly defined larval features (Zimmer and Woollacott, 1993). Based on what little morphological and molecular phylogenetic data exist for the Bryozoa (Dick et al., 2000; Todd, 2000), genera listed under the family Vesiculariidae appear to be a natural grouping resulting from shared descent. However, the disparate morphological traits found in the different larvae of the members of the superfamily Victorelloidea suggest that this superfamily may not be a natural grouping. Based on adult morphological traits, the validity of this superfamily has also been challenged by other authors (e.g., Jebram, 1986).

Among cheilostome bryozoans, there is a clear morphological separation between coronate larval types of ascophoran bryozoans and the larval types of "cellularioid" bryozoans (*Bugula*, *Scrupocellaria*, and others) based on their musculature and the latter larval type's affinity for numerous elongate coronal cells. Based on data presented here, particular cheilostome species with coronate larvae may be united or separated based on the complexity of their large paired retractors, number of coronal cells, and IC patterns. However, testing this hypothesis will require greater taxonomic sampling. Larval traits among the few described cyclostome forms are also conserved, and this is likely the result of morphological canalization due to mass extinction events (Lidgard et al., 1993; McKinney, 1995; Jablonski et al., 1997). Convergent loss of both ciliary and muscular complexity in both cyclostomes and at least one ctenostome bryozoan may be linked to larval forms with limited dispersal capability and divergent reproductive modes. Although pleisiomorphic and derived conditions for larval characters have been proposed by other authors (d'Hondt, 1973; Zimmer and Woollacott, 1993; Zimmer and Reed, 1994), establishing evolutionary polarity among larval forms across bryozoans is complicated by individual species possessing both pleisiomorphic and derived features.

Greater morphological conservation among the macroevolutionary grades of bryozoans is observed for the structure of the presumptive juvenile tissues that form the cystid epithelium at metamorphosis (Lyke et al., 1983). Deriving the cystid solely from the PE is a trait likely shared among several species of victorellid and vesiculariid ctenostome bryozoans with nonfeeding larval forms (Zimmer and Reed, 1994; Santagata, personal observation). However, forming the cystid epithelium from both the PE and IS is found among species of ctenostome and cheilostome bryozoans with cyphonautes larvae as well as cyclostome and most cheilostome bryozo-

ans with nonfeeding larval forms (Prouho, 1890; Nielsen, 1970; Stricker, 1988; Reed, 1991). The larvae of freshwater bryozoans are derived morphologically from those of other bryozoans. Phylactolaemate larvae have an outer epithelium of numerous multiciliated cells that surround a precociously developed ancestrula (Franzén and Sensenbaugh, 1983). This derived pattern is not likely to yield any phylogenetic information for bryozoans as a whole. Overall, deriving the cystid epithelium from dual aboral and oral sources may be pleisiomorphic for all extant bryozoans (Zimmer and Woollacott, 1977b; Reed, 1991). The latter trend has been studied in detail using only traditional histological methods and requires further research on a broader diversity of taxa.

Current molecular phylogenies based on several markers place the Bryozoa along with the annelids, mollusks, brachiopods, and phoronids within the Lophotrochozoa (Halanych, 2004; Passamaneck and Halanych, 2006). Although their position relative to other phyla within the Lophotrochozoa has not been well resolved, it is plausible that the bryozoans occupy a more basal position within this supraphyletic clade (Waeschenbach et al., 2006). Despite the validity of the Lophotrochozoa, there are few larval or adult morphological traits that unite the bryozoans with other lophotrochozoan phyla. This is largely due to the morphological and developmental disparity that exists between the lophophorates and trochozoan phyla as well as the reevaluation of embryological and larval traits often interpreted as lophophorate synapomorphies that are likely the result of convergent selective pressures or bilaterian-wide conservation of particular developmental programs (Santagata, 2004). When considering larval traits, the musculature and cellular arrangements of the feeding cyphonautes form is unique to the bryozoans, with no clear parallel in other phyla. Greater similarities are found among nonfeeding larval forms within the Lophotrochozoa, particularly in the development and morphology of large multiciliated cells used for propulsion. Similar numbers (16) and arrangements of what appear to be primary trochoblast-like cell groups are found during the development the nonfeeding larval forms of kamptozoans (Barrois, 1877; Nielsen, 2005), nemerteans (Maslakova et al., 2004b), bryozoans (Barrois, 1877), and many trochophore larval types (albeit prototrochal cells bear compound cilia, see Nielsen, 2004, 2005). Considering the embryological origin (Zimmer, 1997) and functional plasticity of ciliated cells within bryozoan larvae, it is probable that the morphological similarities shared among the coronal cells of bryozoan larvae and the prototrochal cells of spiralians are the result of convergent functional solutions to swimming in the plankton (Emlet, 1994). However, support for this hypothesis does not conflict with cell specification pathways shared by more closely related trochozoan phyla (Maslakova et al., 2004b), and the possibility that the condition found in bryozoans represents a more basal form of this larval trait. Overall, among the morphological grades of larval bryozoans, the structural variation and arrangement of the main cell groups responsible for ciliary propulsion have been evolutionarily decoupled from the more divergent modifications of larval musculature. The structure of larval ciliary fields reflects the functional demands of swimming and habitat exploration behaviors before metamorphosis, but this is in contrast to the morphology of larval musculature and presumptive juvenile tissues that are linked to macroevolutionary differences in morphogenetic movements during metamorphosis.

ACKNOWLEDGMENTS

I thank the staff of the Smithsonian Marine Station and the staff of Friday Harbor Laboratories. In particular, I thank Valerie Paul, Julie Piraino, Sherry Reed, Mary Rice, Richard Strathmann, Judy Winston, Robert Woollacott, and Russel Zimmer. This paper is contribution number 703 of the Smithsonian Marine Station at Fort Pierce, FL.

LITERATURE CITED

Barrois J. 1877. Recherches sur l'embryologie des Bryozoaires (Memoire sur l'embryologie des Bryozoaires). Trav Stn Zool Wimereux 1:1–305.

Calvet L. 1900. Contributions à l'histoire naturelle des Bryozoaires ectoproctes marins. Trav Inst Zool Univ Montpellier 8:1–488.

d'Hondt JL. 1973. Etude anatomique, histologique, et cytologique de la larve d'*Alcyonidium polyoum* (Hassall, 1841), Bryozoaire Cténostome. Arch Zool Exp Gén 114:537–602.

d'Hondt JL. 1977. Structure larvaire et histogenèse post-larvaire chez *Crisia denticulata* (Lamarck) (Bryozoa, Cyclostomata, Articulata). Zool Scr 6:55–60.

Dick M, Freeland JR, Williams LP, Coggeshall-Burr M. 2000. Use of 16S mitochondrial ribosomal DNA sequences to investigate sister-group relationships among gymnolaemate bryozoans. In: Herrera Cubilla A, Jackson JBC, editors. Proceedings of the 11th International Bryozoology Association Conference. Republic of Panama: Smithsonian Tropical Research Institute. pp 197–210.

Duda TF, Palumbi SR. 1999. Developmental shifts and species selection in gastropods. Proc Natl Acad Sci USA 96:10272–10277.

Emlet RB. 1994. Body form and patterns of ciliation in nonfeeding larvae of echinoderms—Functional solutions to swimming in the plankton. Am Zool 34:570–585.

Franzén A, Sensenbaugh T. 1983. Fine structure of the apical plate in the larva of the fresh-water bryozoan *Plumatella fungosa* (Pallas) (Bryozoa: Phylactolaemata). Zoomorphology 102: 87–98.

Freeman G, Martindale MQ. 2002. The origin of mesoderm in phoronids. Dev Biol 252:301–311.

Gosse PH. 1855. Notes of some new or little-known marine animals. Ann Mag Nat Hist (Ser 2) 16:27–36.

Halanych KM. 2004. The new view of animal phylogeny. Annu Rev Ecol Evol Syst 35:229–256.

Harmer SF. 1915. The Polyzoa of the Siboga Expedition, Part 1: Entoprocta, Ctenostomata, and Cyclostomata. Siboga Expeditie 28a:1–180.

Hart MW, Byrne M, Smith MJ. 1997. Molecular phylogenetic analysis of life-history evolution in asterinid starfish. Evolution 51:1848–1861.

Heller C. 1867. Die Bryozoen des Adriatischen Meeres. Verh zool-bot Ges Wien 17:77–136.

Hinks TH. 1887. The Polyzoa of the Adriatic: A supplement to Professor Heller's "Die Bryozoen des Adriatischen Merees," 1867, Part 2. Ann Mag Nat Hist 19:302–316.

Jablonski D, Lidgard S, Taylor PD. 1997. Comparative ecology of bryozoan radiations: Origin of novelties in cyclostomes and cheilostomes. Palaios 12:505–523.

Jebram DHA. 1986. The ontogenetical and supposed phylogenetical fate of the parietal muscles in the Ctenostomata (Bryozoa). Z Zool Syst Evolforsch 24:58–82.

Jebram DHA. 1992. The polyphyletic origin of the Cheilostomata (Bryozoa). Z Zool Syst Evolforsch 30:46–52.

Jenner RA. 2006. Challenging received wisdoms: Some contributions of the new microscopy to the new animal phylogeny. Integr Comp Biol 46:93–103.

Kupelwieser H. 1905. Untersuchungen uber den feineren Bau und die metamorphose des Cyphonautes. Zoologica (Stuttgart) 19:1–50.

Lidgard S, McKinney FK, Taylor PD. 1993. Competition, clade replacement, and a history of cyclostome and cheilostome bryozoan diversity. Paleobiology 19:352–371.

Linnaeus C. 1758. Systema Naturae, 10th ed. Stockholm. Vol. 1. Holmiae: L. Salvii. pp 789–821.

Linnaeus C. 1767. Systema Naturae, 12th ed. Holmiae: L. Salvii. pp 1–1327.

Lyke EB, Reed CG, Woollacott RM. 1983. Origin of the cystid epidermis during the metamorphosis of three species of gymnolaemate bryozoans. Zoomorphology 102:99–110.

Maslakova SA, Martindale MQ, Norenburg JL. 2004a. Fundamental properties of the spiralian developmental program are displayed by the basal nemertean *Carinoma tremaphoros* (Palaeonemertea, Nemertea). Dev Biol 267: 342–360.

Maslakova SA, Martindale MQ, Norenburg JL. 2004b. Vestigial prototroch in a basal nemertean, *Carinoma tremaphoros* (Nemertea; Palaeonemertea). Evol Dev 6:219–226.

McDougall C, Chen W-C, Shimeld SM, Ferrier DK. 2006. The development of the larval nervous system, musculature and ciliary bands of *Pomatoceros lamarckii* (Annelida): Heterochrony in polychaetes. Front Zool 3:1–14.

McEdward LR, Janies DA. 1993. Life cycle evolution in asteroids: What is a larva? Biol Bull 184:255–268.

McKinney FK. 1995. One hundred million years of competitive interactions between bryozoan clades: Asymmetrical but not escalating. Biol J Linn Soc Lond 56:465–481.

Milne-Edwards H. 1838. Mémoire sur les Crisies, les Hornères et plusieurs autres polypes vivans ou fossiles dont l'organisation est analogue à celle des Tubulipores. Ann Sci Nat (Ser 2) Zool 9:193–238.

Nielsen C. 1970. On metamorphosis and ancestrula formation in cyclostomatous bryozoans. Ophelia 7:217–256.

Nielsen C. 2004. Trochophora larvae: Cell-lineages, ciliary bands, and body regions, Part 1: Annelida and mollusca. J Exp Zool Part B 302:35–68.

Nielsen C. 2005. Trochophora larvae: Cell-lineages, ciliary bands and body regions, Part 2: Other groups and general discussion. J Exp Zool Part B 304:401–447.

Nützel A, Lehnert O, Fryda J. 2006. Origin of planktotrophy: Evidence from early molluscs. Evol Dev 8:325–330.

Osburn RC. 1914. Bryozoa of the Tortugas islands. Carnegie Inst Washington 182:181–222.

Page LR. 1998. Sequential developmental programmes for retractor muscles of a caenogastropod: Reappraisal of evolutionary homologues. Proc R Soc Lond B Biol Sci 265:2243–2250.

Passamaneck Y, Halanych KM. 2006. Lophotrochozoan phylogeny assessed with LSU and SSU data: Evidence of lophophorate polyphyly. Mol Phylogenet Evol 40:20–28.

Prouho H. 1890. Recherches sur la larve de *Flustrella hispida*: Structure et métamorphose. Arch Zool Exp Gén 2 (Sér 8):409–459.

Prouho H. 1892. Contribution à l'histoire des bryozoaires. Arch Zool Exp Gén 2 Sér 10:557–656.

Raff RA, Byrne M. 2006. The active evolutionary lives of echinoderm larvae. Heredity 97:244–252.

Reed CG. 1984. Larval attachment by eversion of the internal sac in the marine bryozoan *Bowerbankia gracilis* (Ctenostomata, Vesicularioidea): A muscle mediated morphogenetic movement. Acta Zool 65:227–238.

Reed CG. 1988. Organization of the nervous system and sensory organs in the larva of the marine bryozoan *Bowerbankia gracilis* (Ctenostomata, Vesicularidae): Functional significance of the apical disc and pyriform organ. Acta Zool 69:177–194.

Reed CG. 1991. Bryozoa. In: Giese AC, Pearse JS, editors. Reproduction of Marine Invertebrates, Vol. 6: Echinoderms and Lophophorates. Pacific Grove, CA: The Boxwood Press. pp 85–245.

Reed CG, Cloney RA. 1982a. The larval morphology of the marine bryozoan *Bowerbankia gracilis* (Ctenostomata, Vesicularioidea). Zoomorphology 100:23–54.

Reed CG, Cloney RA. 1982b. The settlement and metamorphosis of the marine bryozoan *Bowerbankia gracilis* (Ctenostomata, Vesicularioidea). Zoomorphology 101:103–132.

Reed CG, Woollacott RM. 1982. Mechanisms of rapid morphogenetic movements in the metamorphosis of the bryozoan *Bugula neritina* (Cheilostomata, Cellularioidea), Part 1: Attachment to the substratum. J Morphol 172:335–348.

Reed CG, Ninos JM, Woollacott RM. 1988. Bryozoan larvae as mosaics of multifunctional ciliary fields: Ultrastructure of the sensory organs of *Bugula stolonifera* (Cheilostomata, Cellularioidea). J Morphol 197:127–145.

Ryland JS. 1960. The British species of *Bugula* (Polyzoa). Proc Zool Soc Lond 134:65–105.

Ryland JS, Porter ME. 2006. The identification, distribution, and biology of encrusting species of *Alcyonidium* (Bryozoa: Ctenostomatida) around the coasts of Ireland. Biol Environ Proc R Ir Acad B 106:19–33.

Santagata S. 2002. Structure and metamorphic remodeling of the larval nervous system and musculature of *Phoronis pallida* (Phoronida). Evol Dev 4:28–42.

Santagata S. 2004. Larval development of *Phoronis pallida* (Phoronida): Implications for morphological convergence and divergence among larval body plans. J Morphol 259:347–358.

Santagata S, Zimmer RL. 2000. Comparing cell patterns of coronate bryozoan larvae with fluorescent probes. In: Herrera Cubilla A, Jackson JBC, editors. Proceedings of the 11th International Bryozoology Association Conference. Republic of Panama: Smithsonian Tropical Research Institute. pp 365–375.

Santagata S, Zimmer RL. 2002. Comparison of the neuromuscular systems among actinotroch larvae: Systematic and evolutionary implications. Evol Dev 4:43–54.

Strathmann RR, Eernisse DJ. 1994. What molecular phylogenies tell us about the evolution of larval forms. Am Zool 34:502–512.

Stricker SA. 1988. Metamorphosis of the marine bryozoan *Membranipora membranacea*: An ultrastructural study of rapid morphogenetic movements. J Morphol 196:53–72.

Stricker SA, Reed CG, Zimmer RL. 1988a. The cyphonautes larva of the marine bryozoan *Membranipora membranacea*, Part 1: General morphology, body wall, and gut. Can J Zool 66:368–383.

Stricker SA, Reed CG, Zimmer RL. 1988b. The cyphonautes larva of the marine bryozoan *Membranipora membranacea*, Part 2: Internal sac, musculature, and pyriform organ. Can J Zool 66:384–398.

Taylor PD. 1988. Major radiation of cheilostome bryozoans: Triggered by the evolution of a new larval type? Hist Biol 1:45–64.

Taylor PD. 1990. Bioimmured ctenostomes from the Jurassic and the origin of the cheilostome Bryozoa. Palaeontology 33:19–34.

Tessmar-Raible K, Arendt D. 2003. Emerging systems: Between vertebrates and arthropods, the Lophotrochozoa. Curr Opin Genet Dev 13:331–340.

Todd JA. 2000. The central role of ctenostomes in bryozoan phylogeny. In: Herrera Cubilla A, Jackson JBC, editors. Proceedings of the 11th International Bryozoology Association Conference. Republic of Panama: Smithsonian Tropical Research Institute. pp 104–135.

Van den Biggelaar JAM, Dictus W, van Loon AE. 1997. Cleavage patterns, cell-lineages, and cell specification are clues to phyletic lineages in Spiralia. Semin Cell Dev Biol 8:367–378.

Waeschenbach A, Telford MJ, Porter JS, Littlewood DTJ. 2006. The complete mitochondrial genome of *Flustrellidra hispida* and the phylogenetic position of Bryozoa among the Metazoa. Mol Phylogenet Evol 40:195–207.

Wanninger A, Koop D, Degnan BM. 2005. Immunocytochemistry and metamorphic fate of the larval nervous system of *Triphyllozoon mucronatum* (Ectoprocta: Gymnolaemata: Cheilostomata). Zoomorphology 124:161–170.

Winston JE. 2005. Re-description and revision of Smitt's "Floridan Bryozoa" in the Collection of the Museum of Comparative Zoology, Harvard University. Virginia Museum of Natural History Memoir Number 7:1–148.

Woollacott RM, Zimmer RL. 1971. Attachment and metamorphosis of the cheilo-ctenostome bryozoan *Bugula neritina*. J Morphol 134:351–382.

Woollacott RM, Zimmer RL. 1972. Fine structure of a potential photoreceptor organ in the larva of *Bugula neritina* (Bryozoa). Z Zellforsch Mikrosk Anat 123:458–469.

Wray GA. 2002. Do convergent developmental mechanisms underlie convergent phenotypes? Brain Behav Evol 59:327–336.

Zimmer RL. 1997. Phoronids, brachiopods, and bryozoans, the lophophorates. In: Gilbert SF, Raunio AM, editors. Embryology: Constructing the Organism. Sunderland, MA: Sinauer Associates. pp 279–305.

Zimmer RL, Reed CG. 1994. Morphology and ultrastructure of the larva of the bryozoan *Tanganella muelleri* (Ctenostomata: Victorellidae). In: Wilson WH, Stricker SA, Shinn GL, editors. Reproduction and Development of Marine Invertebrates. Baltimore, London: The Johns Hopkins University Press. pp 224–245.

Zimmer RL, Woollacott RM. 1977a. Structure and classification of bryozoan larvae. In: Woollacott RM, Zimmer RL, editors. The Biology of Bryozoans. New York: Academic Press. pp 57–89.

Zimmer RL, Woollacott RM. 1977b. Metamorphosis, ancestrulae, and coloniality in bryozoan life cycles. In: Woollacott RM, Zimmer RL, editors. The Biology of Bryozoans. New York: Academic Press. pp 91–142.

Zimmer RL, Woollacott RM. 1989a. Larval morphology of the bryozoan *Watersipora arcuata* (Cheilostomata: Ascophora). J Morphol 199:125–150.

Zimmer RL, Woollacott RM. 1989b. Intercoronal cell complex of larvae of the bryozoan *Watersipora arcuata* (Cheilostomata: Ascophora). J Morphol 199:151–164.

Zimmer RL, Woollacott RM. 1993. Anatomy of the larva of *Amathia vidovici* (Bryozoa: Ctenostomata) and phylogenetic significance of the vesicullariform larva. J Morphol 215:1–29.